

Short Communication

## A Label-free ECL Biosensor for The Detection of Uric Acid Based on Au NRs@TiO<sub>2</sub> Nanocomposite

Meng Jiang<sup>1,\*</sup>, Jing-Shuai Chen<sup>2</sup>

<sup>1</sup> Department of Laboratory Medicine, The First Affiliated Hospital of Anhui Medical University, Hefei 230032, China

<sup>2</sup> School of Chemistry & Chemical Engineering, Anhui University, Hefei 230601, China

\*E-mail: [jiangmeng401@163.com](mailto:jiangmeng401@163.com)

Received: 3 September 2018 / Accepted: 13 December 2018 / Published: 7 February 2019

---

A novel ultrasensitive electrochemiluminescence (ECL) biosensor was developed to detect uric acid (UA) based on Au NRs@TiO<sub>2</sub> nanocomposite. The Au NRs@TiO<sub>2</sub> nanocomposite was successfully prepared. The morphologies of Au NRs@TiO<sub>2</sub> nanocomposite were observed by scanning electron microscope (SEM), transmission electron microscopy (TEM). Morphological representation results showed that the nanomaterials were well dispersed and had a uniform surface. The characterization of electrochemiluminescence properties indicated that the Au NRs@TiO<sub>2</sub> possessed good ECL behavior. The Au NRs@TiO<sub>2</sub> nanocomposite was used to establish a highly sensitive electrochemiluminescence biosensor for the uric acid. A highly sensitive and selective electrochemiluminescence biosensor was established successfully which based on the Au NRs@TiO<sub>2</sub> nanocomposite. Under the optimal conditions, the biosensor shown a wide calibration range from 40 nM to 28 μM (R = 0.9985) with detection limit of 15 nM. The proposed electrochemiluminescence biosensor provided selective detection of uric acid range from 40 nM to 28 μM (R = 0.9985) with detection limit of 15 nM. This biosensor exhibited stable, sensitive and reproducible detection of uric acid, and was able to be used in clinical detection.

---

**Keywords:** Au NRs@TiO<sub>2</sub>; electrochemiluminescence; uric acid; biosensor

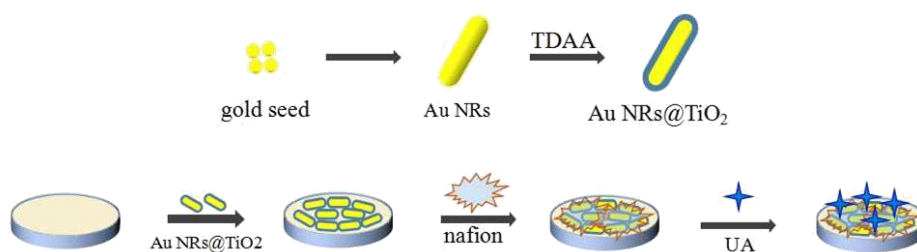
### 1. INTRODUCTION

Uric acid is the principle final product of the purine metabolism [1, 2]. Under normal circumstances, uric acid is about 1200 mg in the body, which produces about 600 mg of a day, and at the same time excreted to reach the balance. Once the body's balance of uric acid is destroyed, it will cause a series of diseases such as hypouricemia, kidney damage, gout, cardiac problem, Lesch-Nyhan

syndrome, leading frequently to multiple sclerosis [3-9]. It is necessary to point out that unhealthy diet, unenough exercise and wrongly use of drugs will lead to the higher level of uric acid. Hence, it is necessary to find a sensitive method to precisely detect the uric acid.

Recently, a lot of approaches have been developed for the detection of uric acid, such as high performance liquid chromatographic (HPLC) [10-12], chromatography [13, 14], spectrophotometry [15, 16], electrochemical methods [17, 18] and so on. Compared with these high-cost, time-consuming and complex method, electrochemiluminescence (ECL) has obvious advantages. ECL possesses the advantages of chemiluminescence and electrochemistry simultaneously, which is suit for sensitive detection of low level model analysis in complex matrices with low background signal and simplified optical setup [19, 20]. In recent years, ECL of nanomaterials have attracted great interest in biosensor. Among them, CdSe, CdS, and PbS nanocrystals have been used as ECL emitters because of their high quantum yield, excellent photostability and narrow emission. The presence of heave metal in a high performance semiconductor nanocrystals is necessary. However, these heavy metals will cause a critical health hazard and environment. The development of the environmentally benign, low-toxicity or nontoxic ECL emitters has received lots of attentions. Gold nanomaterial is one of the most widely used because of their unique physicochemical properties such as good conductivity, non-toxicity, large surface-to-volume ratio and biocompatibility [21-24]. In this paper, the ECL properties of Au NRs were studied, and then the Au NRs were used to construct sensitive ECL biosensor.

A sensitive and precise biosensor based on the Au NRs@TiO<sub>2</sub> nanocomposite was successfully prepared for the detection of uric acid. The Au NRs@TiO<sub>2</sub> were then used for ECL. The result of ECL analysis revealed that the nanocomposite can produce a stable and high intensity luminescence under certain potential condition. The ECL biosensor based on Au NRs@TiO<sub>2</sub> nanocomposite was able to detect uric acid rapidly, accurately, and stable. Under the optimal conditions, the uric acid detection range was from 40 nM to 28  $\mu$ M and the detection limit was 15 nM.



**Scheme 1.** The stepwise fabrication process of ECL biosensor.

## 2. EXPERIMENTAL

### 2.1. Chemical and materials

Chloroauric acid (HAuCl<sub>4</sub>), sodium borohydride (NaBH<sub>4</sub>), silver nitrate (AgNO<sub>3</sub>), sodium hydroxide (NaOH) and potassium peroxydisulfate (K<sub>2</sub>S<sub>2</sub>O<sub>8</sub>) were obtained from Sinopharm Chemical

Reagent Co., Ltd. Titanium diisopropoxide bis (acetylacetonate) (TDAA) was purchased from Aladdin reagent Co., Ltd, Uric acid (UC), ascorbic acid and Nafion were purchased from Shanghai Sangon Biotech Co., Ltd. All reagents were used directly. Phosphate buffered solutions (PBS) was prepared with  $\text{NaH}_2\text{PO}_4$  and  $\text{Na}_2\text{HPO}_4$ , and adjusting the pH with NaOH and  $\text{H}_3\text{PO}_4$ . PBS (pH=7.4) containing  $0.1 \text{ mol}\cdot\text{L}^{-1} \text{ K}_2\text{S}_2\text{O}_8$  and  $0.1 \text{ mol}\cdot\text{L}^{-1} \text{ KCl}$  was used as the electrolyte in ECL test. Deionized water was used throughout this work (electrical resistivity  $\geq 18 \Omega$ ).

## 2.2. Apparatus

The morphology and structural of the Au NRs@TiO<sub>2</sub> were measured by field emission scanning electron microscopy (SEM, S4800, Hitachi, Japan) and transmission electron microscopy (TEM, JEM-2100, JEOL, Japan). The electrochemical and electrochemiluminescence experiments were carried out with electrochemistry work station (CHI 660D CH Instrument Co., China) and electrochemiluminescence analyzer (MPI-A, Xi'An Remax Electronic Science & Technology Co. Ltd., China) with a conventional three-electrode system composed of a platinum wire as the auxiliary electrode, a Ag/AgCl electrode as the reference and GCE as the working electrodes. Electrochemical impedance spectra (EIS) were characterized by a Thales electrochemical workstation (Zahner-elektrik GmbH & Co. KG, Germany).

## 2.3. Synthesis of Au NRs

The Au NRs were synthesized based on the seed-mediated growth method reported in the literature [25]. The synthesis process consists of two steps: firstly, 2.5 mL HAuCl<sub>4</sub> (1 mM) was added to 5 mL CTAB (0.2 M). The solution was orange. Then 600  $\mu\text{L}$  NaBH<sub>4</sub> (10 mM) was added in the solution. After 5 min, the orange was reduced, and the gold seeds solution was synthesized. Next, 2.5 mL of HAuCl<sub>4</sub> was added to 2.5 mL of Cetyltrimethylammonium bromide (CTAB), then the mixture consisting of 113  $\mu\text{L}$  of AgNO<sub>3</sub> (4 mM) and 35  $\mu\text{L}$  of ascorbic acid (78.8 mM) was dropped into the above solution. After a mild shock, a clear solution was formed. Then 4  $\mu\text{L}$  of gold seeds solution was dropped in the clear solution and then reacted for 2 h.

## 2.4. The preparations of Au NRs@TiO<sub>2</sub>

CTAB (80  $\mu\text{L}$ , 0.01 M) was first added into 1620  $\mu\text{L}$  H<sub>2</sub>O. The as-prepared Au nanorod solution (300  $\mu\text{L}$ ) was dispersed in the solution and followed by vibrating for 10 min. 8  $\mu\text{L}$  of NaOH (0.01 M) was then added and followed by vibrating for another 10 min. After that, 1  $\mu\text{L}$  of Titanium diisopropoxide bis (acetyl acetate) (TDAA, 1% in methanol) was added into the above mixture and followed by continuous vibrating. Another 1  $\mu\text{L}$  of TDAA (1% in methanol) was added every 30 min till the total volume of TDAA is 4  $\mu\text{L}$ . The resultant Au@TiO<sub>2</sub> nanostructure solution was centrifuged and re-dispersed into water (1 mL).

### 2.5. Fabrication of ECL sensor

Scheme 1 showed the preparation process of the ECL biosensor. The whole process can be divided into two sections. Firstly, the surface of glass carbon electrode (GCE,  $d=4\text{mm}$ ) was polished carefully to the mirror state by 1.0, 0.3, and 0.05  $\mu\text{m}$  alumina powder and then sonicated by ethanol and distilled water for 30 s respectively. Secondly, 10  $\mu\text{L}$  Au@TiO<sub>2</sub> nanocomposites solution was dropped onto GCE to form the Au@TiO<sub>2</sub> electrode. Then 3  $\mu\text{L}$  of Nafion solution (0.1 wt%) was dropped onto the above modified electrode and dried in air.

### 2.6. Electrochemiluminescence analysis

ECL measurement was performed in the PBS buffer (pH=7.4) which contains 0.1 M KCl, 0.1 M K<sub>2</sub>S<sub>2</sub>O<sub>8</sub> and different concentrations of uric acid. The working potential was from 0V to -1.5V with a scan rate of 300 mV/s.

## 3. RESULT AND DISCUSSION

### 3.1. Characterization of Au NRs@TiO<sub>2</sub> core-shell nanostructures

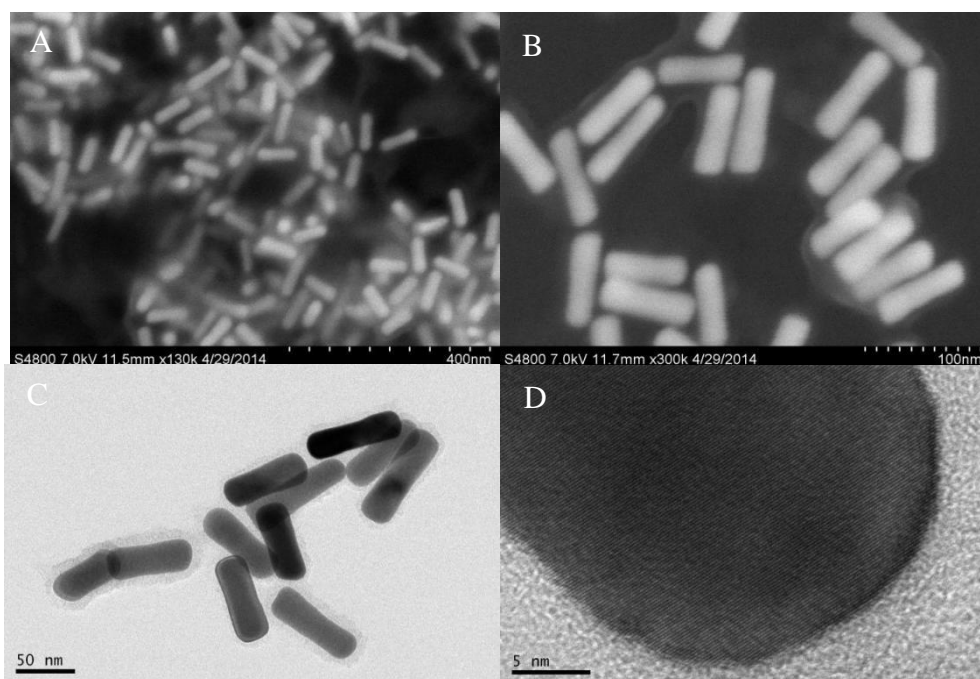
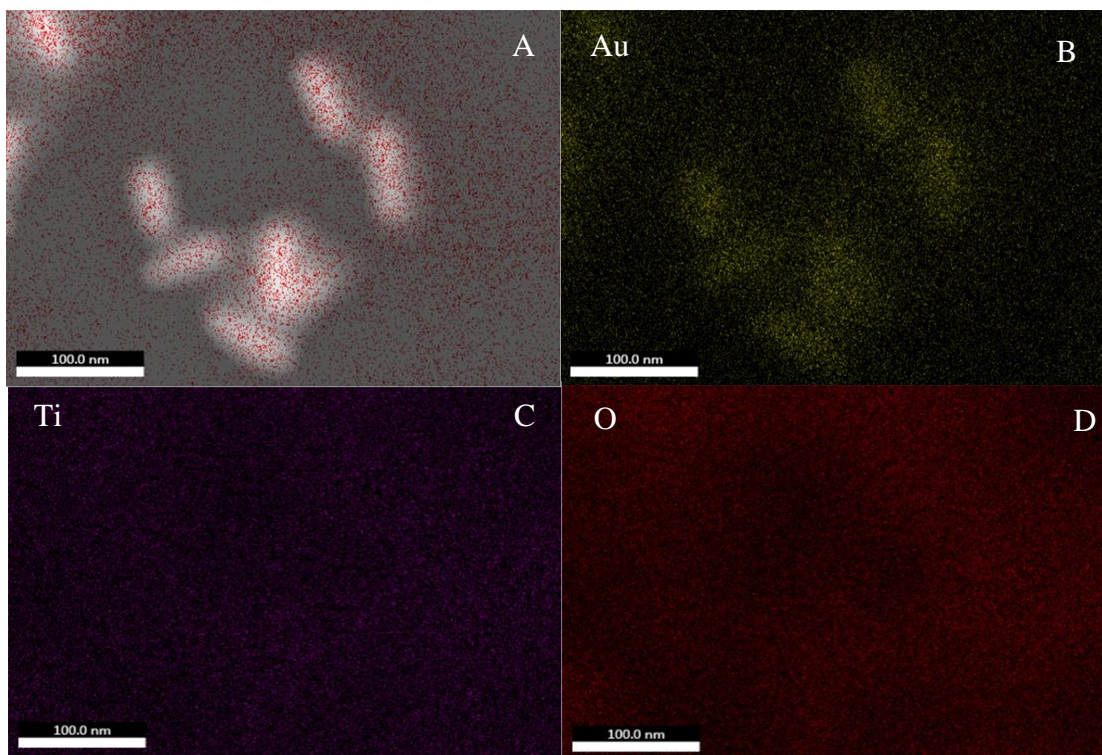


**Figure 1.** SEM of the Au NRs@TiO<sub>2</sub> (A) and (B), TEM of the Au NRs@TiO<sub>2</sub> (C), HRTEM of Au NRs@TiO<sub>2</sub> (D).

The morphologies and size of the as-prepared nanocomposites were illustrated by SEM and TEM techniques. As shown in the typical SEM image (Fig. 1A, Fig. 1B) the Au NRs were coated by TiO<sub>2</sub> and the Au NRs had a uniform size. The average diameter and length of the Au@TiO<sub>2</sub> core-shell nanostructures were 20 nm and 90 nm, respectively. From high magnification TEM images (inset Fig. 1C), it was observed that the average thickness of the TiO<sub>2</sub> shell were 5 nm and the Au NRs@TiO<sub>2</sub> was

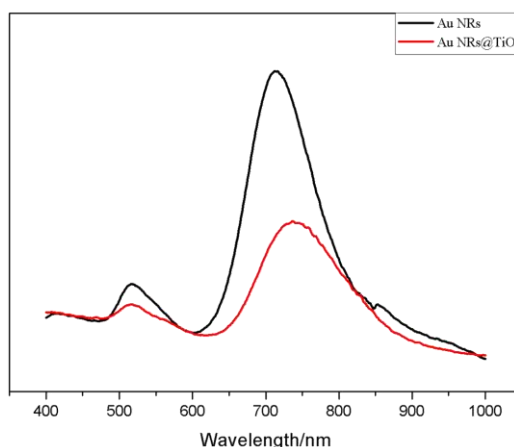
uniform in appearance. Lattice fringe of the Au NRs was clear and distinct from the HR-TEM image (Fig. 1D), which denoted the (111) face of Au NRs [25]. Comprehensive analysis of the SEM and TEM images, the Au NRs@TiO<sub>2</sub> possessed a rod-shaped and a mean size.

To further confirm the Au NRs was coated by TiO<sub>2</sub> shell, the ultra-high resolution scanning electron microscope imaging in conjunction with energy-dispersive X-ray spectrum (EDX) elemental mapping are exhibited in Figure 2. The Au NRs are monodisperse and process a uniform appearance in Fig. 2A and 2B. The Fig. 2C and 2D reveal that the shell was composed of Ti and O.



**Figure 2.** EDX elemental maps of (A) elements overlay, (B) Au, (C) Ti, (D) O.

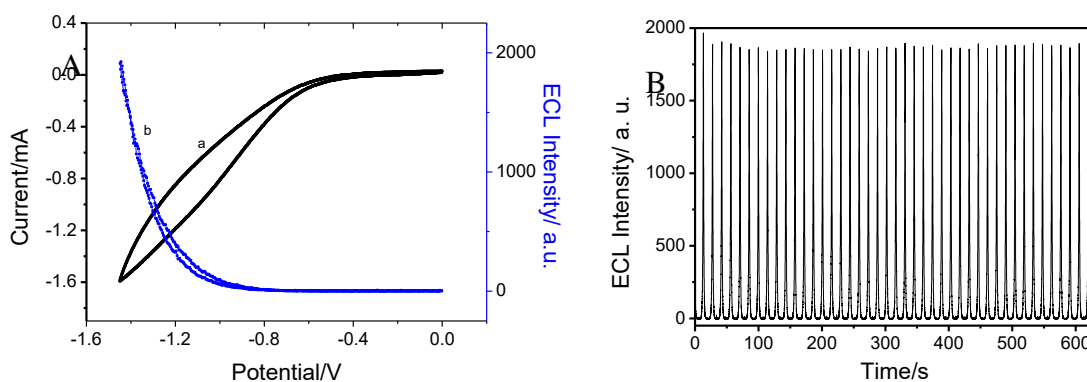
As shown in the UV-Vis absorption spectra (Figure 3), the transverse and longitudinal localized surface plasmon resonance (LSPR) mode of the uncoated Au NRs are 517 nm and 714 nm, respectively. The LSPR wavelength is very sensitive to the environments surrounding the nanorods especially the longitudinal LSPR. Therefore, after coated by TiO<sub>2</sub> shell, the longitudinal LSPR band of Au NRs was red-shift and broadened slightly from 714 nm to 738 nm.



**Figure 3.** The extinction spectra of the Au NRs and Au NRs@TiO<sub>2</sub>.

### 3.2. ECL behavior of the Au NRs@TiO<sub>2</sub>

**A**



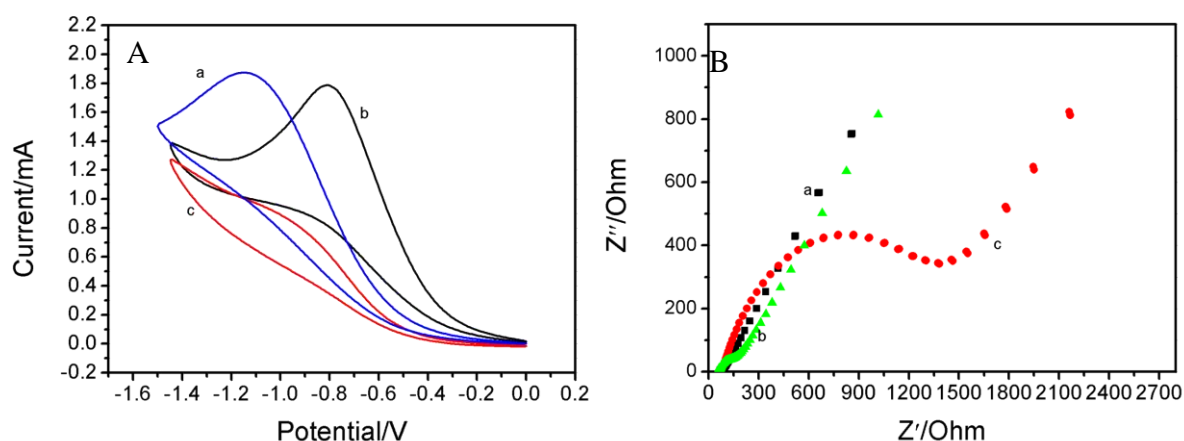
**Figure 4.** (A) Cycle voltammogram (a) and ECL intensity-potential curves (b). (B) Stability of the ECL signals of Au NRs@TiO<sub>2</sub> nanocomposites scanning from 0 to -1.5 V in 0.1 M PBS (pH=7.4) containing 0.1 mol L<sup>-1</sup> S<sub>2</sub>O<sub>8</sub><sup>2-</sup>.

Fig. 4A showed the ECL-potential and CV curves obtained by the Au NRs@TiO<sub>2</sub> modified electrodes. The Au NRs@TiO<sub>2</sub> showed good ECL behavior (Fig. 4B). The electron-transfer annihilation of electrogenerated anion and cation radicals will generate the excited-state molecules, and then the excited-state molecules release luminescence. This chemiluminescence process is defined as electrochemiluminescence. Figure 4B showed the ECL emission of the Au NRs@TiO<sub>2</sub> nanocomposites under subsequent potential scans from 0 to -1.5 V for 30 cycles. The highly and stably ECL signals suggest that the Au NRs@TiO<sub>2</sub> nanocomposites was suitable for ECL detection. According to the literature[26], when the metal nanoparticles contact with a charged semiconductor such as TiO<sub>2</sub>, the Fermi levels of the two materials equilibrate and the metals will accept the charges which transfer from the conduction band of the excited TiO<sub>2</sub>. Thus TiO<sub>2</sub> could used as an intensifier for ECL sensor. In this system, the ECL was emitted by the concomitant reduction of Au NRs and S<sub>2</sub>O<sub>8</sub><sup>2-</sup> which was similar to

that of Au NCs[27]. Firstly, the Au NRs were reduced to Au NRs<sup>-</sup>, while the coreactant S<sub>2</sub>O<sub>8</sub><sup>2-</sup> was reduced to the strong oxidant SO<sub>4</sub><sup>-</sup>. Then the excited state species (Au NRs<sup>\*</sup>) were produced by the reacting Au NRs<sup>-</sup> with SO<sub>4</sub><sup>-</sup> on the surface of the electrode. Finally Au NRs<sup>\*</sup> emitted light and jumped to ground state.

### 3.3. EIS characterization of the biosensor

The modified electrode surface was measured by cyclic voltammogram (CV) and electrochemical impedance spectroscopy (EIS). The CV responses of different modified electrode in 5.0 mM of [Fe(CN)<sub>6</sub>]<sup>3-/4-</sup> solution were shown in Fig. 5A. The current of bare electrode was significantly higher than other modified electrodes (curve a). After the Au NRs@TiO<sub>2</sub> modified on the electrode, the current was slightly decreased (curve b). The decreased current may caused by TiO<sub>2</sub>, which is a typical semi-conductor[28]. The process of the electron transfer between the electrode and the [Fe(CN)<sub>6</sub>]<sup>3-/4-</sup> was impeded. The current decreased significantly after Nafion was modified on the electrode (curve c) because the Nafion hindered the electron transfer. EIS is an effective method to illustrate the fabrication process of the ECL biosensor. The semicircular portion of the impedance spectra is corresponding to the electron-transfer-limited and the linear portion represent the diffusion process[29]. As shown in the Fig. 5B, the change of the EIS for the entire surface modification of the electrode was declared. The bare electrode was confirmed that possess an excellent electronic conduction capability ulteriorly (curve a). When the Au NRs@TiO<sub>2</sub> loaded on the electrode, the electronic conduction capability decreased slightly (curve b) due to the semiconductor property of the TiO<sub>2</sub>. The diameter increased obviously when Nafion was dripped on the surface of electrode (curve c). Those results indicated that the biosensor was fabricated successfully.



**Figure 5.** The curve of CVs (A) and EIS (B) for the stepwise electrode modification process measure in 5.0 mM [Fe(CN)<sub>6</sub>]<sup>3-/4-</sup> containing 0.1 M KCl and with the scan range of 0--1.6 V at the rate of 100 mV/s. (a) bare GCE, (b) Au NRs@TiO<sub>2</sub>/GEC, (c) Nafion/Au NRs@TiO<sub>2</sub>/GCE.

### 3.4. Optimization of the experimental condition

In order to optimize performance of the prepared biosensor, several experimental parameters including the scan rate, the concentration of Nafion, pH value and the concentration of  $K_2S_2O_8$  were considered. For the purpose of getting the optimal ECL response, the scan rate in the range of 0.1-0.5 V/s was studied. The impact of pH value was investigated in the range of 5.0~9.0. As shown in Fig. 6A, the intensity of ECL was significantly enhanced with scan rate from 0.1 V/s to 0.2 V/s. Then the intensity of ECL was decreased as the scan rate increases. Hence, the best scan rate was 0.2 V/s. As shown in Fig. 6B, the ECL intensity increased with the pH value in the range from 4.0 to 7.4. This may be explained that the more negative charged species promotes the transfer process of electrons. However, when the pH value exceeded 7.4, the intensity of ECL decreased, which suggested that excessive anions made the ECL intensity decrease rapidly. Thus 7.4 was the optimal pH value for this system. This may be caused by that the negatively charged species can accelerate electron transfer. Excessive anions would loaded on the surface of the electrode when the pH was higher than 7.4. And then the load of  $Au@TiO_2$  was suppressed[30].

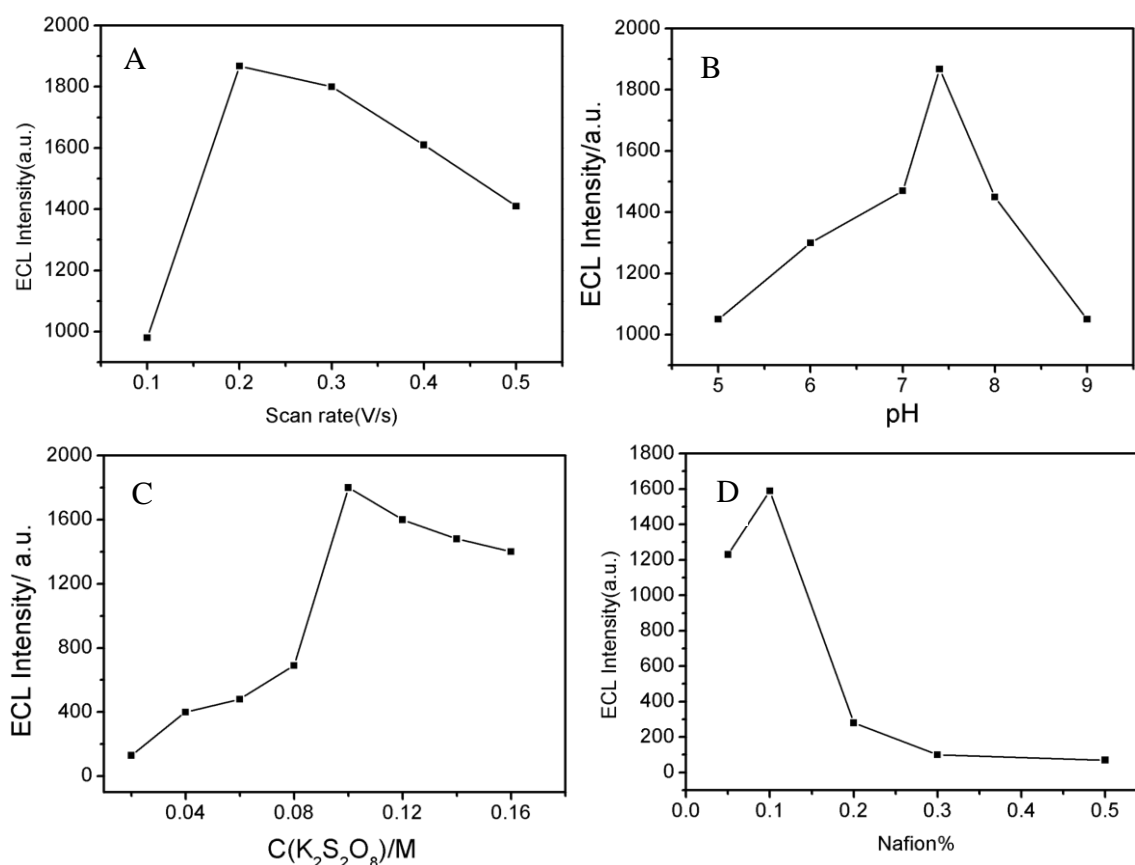


**Figure 6.** Effects of experiment parameters on the ECL response: (A) the scan rate, (B) the pH value, and (C) the  $K_2S_2O_8$  concentration, (D) the nafion concentration.

The effect of  $K_2S_2O_8$  concentration was optimized at the range from 0.02 M to 0.16 M (Fig. 4C). In Fig. 6C, the ECL intensity firstly increased, which suggested that that the more oxidant led to

increase of the ECL intensity. After  $K_2S_2O_8$  was higher than 0.1 M, the ECL intensity decreased, which suggested that the excessive  $SO_4^{\cdot-}$  increased the film thickness. Finally the 0.1 M  $K_2S_2O_8$  was selected. The concentration of Nafion is a significant factor for the biosensor. As described in Fig. 6D, the optimal ECL intensity was 0.1%. After the concentration of Nafion exceeds 0.1%, the ECL intensity decreased with the increase of the concentration of Nafion.

### 3.5. ECL analysis of the uric acid biosensor

The Au NRs@TiO<sub>2</sub> nanocomposites were used to make up the ECL biosensor for the detection of uric acid. In order to evaluate the ability the ECL biosensor, uric acid standards of different concentration were tested on the basis of the developed protocol. The concentration of uric acid in the buffer directly affected the ECL intensity. The intensity of ECL decreased as the concentration of the uric acid increased. The steric hindrance increased by uric acid inhabit the transfer of electrons and  $K_2S_2O_8$  in the ECL reaction. Thus the ECL intensity decreased. The results indicated that the UA concentration could be accurately determined by this ECL sensor. Figure 7 showed the ECL intensity for a range of different concentrations of uric acid. The ECL response signal decreased in a linear manner with the UA concentration range from 40 nM to 28  $\mu$ M, where the linear equation was:  $I_{ECL} = 6.5123 \times 10^{-4}C(UA) + 1.03778$ . The regression equation coefficient was 0.9985. The limit of the detection was 15 nM. Compared with previously reported methods for the detection of UA [31-38] in Table 1, this proposed biosensor had a broad linear range and lower detection, which may be ascribed to the excellent electron transfer activity of Au NRs@TiO<sub>2</sub> nanocomposite. It can be deduced that the proposed biosensor exhibit excellent performance in the detection of UA.

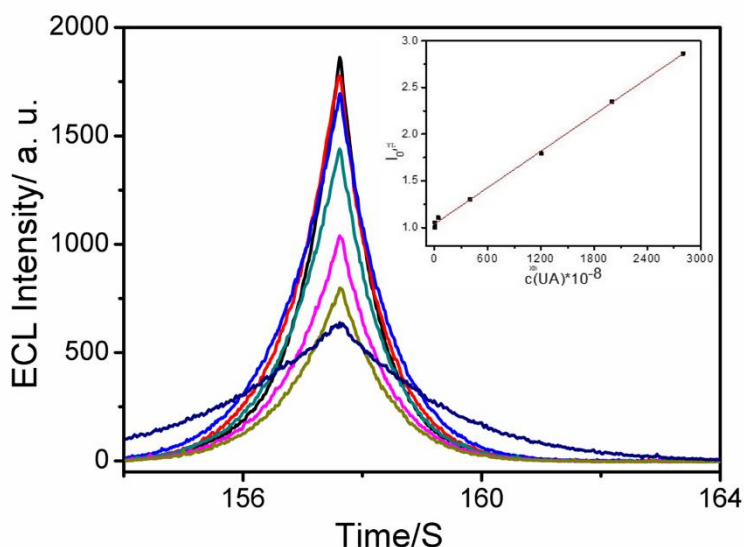


**Figure 7.** ECL response and the corresponding calibration curve of the biosensor for the detection of different concentrations of uric acid from 40 nM to 28  $\mu$ M in the internal.

**Table 1.** Comparison of UA determination using the previously reported methods.

Reagent	Method	Linear range	LOD	Reference
Au@Polyluminol nanoflowers	ECL	3.0-300 $\mu\text{M}$	1.00 $\mu\text{M}$	[31]
$\text{Fe}_3\text{O}_4$ @ $\text{SiO}_2$ /grapheme nanocomposites	DPV	0.5-250.0 $\mu\text{M}$	0.07 $\mu\text{M}$	[32]
$\text{Ag}_3\text{Fe}(\text{CN})_6$ -GR	Amperometry	2.0-80.0 $\mu\text{M}$	0.07 $\mu\text{M}$	[33]
$\text{Tb}^{\text{III}}$ -dtpa-bis(2,6-diaminopurine) (Tb-dtpa-bdap)	Fluorescent	10.0-50 $\mu\text{M}$	5.80 $\mu\text{M}$	[34]
Graphene flakes and platinum nanoparticles	cyclic voltammetry	60.0-288.0 $\mu\text{M}$	18.00 $\mu\text{M}$	[35]
Three-dimensional porous graphene	DPV	0.14-464.0 $\mu\text{M}$	1.0 $\mu\text{M}$	[36]
Graphitic carbon nitride (g- $\text{C}_3\text{N}_4$ ) nanosheets	DPV	5.0-189.0 $\mu\text{M}$	0.5 $\mu\text{M}$	[37]
poly(diallyldimethylammonium chloride) and graphene oxide	DPV	0.25-1500.0 $\mu\text{M}$	0.08 $\mu\text{M}$	[38]
Au NRs@ $\text{TiO}_2$ nanocomposites	ECL	0.04-280 $\mu\text{M}$	0.015 $\mu\text{M}$	This work

### 3.6. Repeatability, specificity and stability of the biosensor

In this test, the responsive specificity of the ECL sensor were investigated. Four glassy carbon electrodes were prepared for the responsive signal of uric acid whose concentration was  $4 \times 10^{-6}$  M in the solution and the relative standard deviation was 0.304%, which indicated the sensor possessed good repeatability. During this test, the specificity and the stability were also investigated. We measured the selectivity of four electrodes for measurement of uric acid, and each electrode was respectively with the same concentration of ascorbic acid and dopamine solution as the interfering substances. The relative standard deviation of four electrodes compared with pure uric acid respectively was 0.7874%, 0.5172%, 0.9633%, 0.7119% and the average relative standard deviation is 0.7450%. This indicated that the sensor had good specificity. In addition, the sensor was put in the refrigerator of 4 °C and was preserved for 14 days. Then the electrochemiluminescence response of uric acid solution were detected. The results showed that the luminescence intensity didn't change obviously, indicating the good stability of the obtained sensor.

### 3.7 Application in detection of real samples

Colorimetric method is the gold standard method. The proposed biosensor was compared with colorimetric method by estimating UA in human serum samples. The relative deviation between these two methods was from -2.49% to 7.57% (shown in Table 2), indicating an acceptable accuracy of the assay in analysing clinical samples.

**Table 2.** Comparison of UA determinations in human serum samples using the proposed method and colorimetric method (Average value from five successive measurements).

Serum samples	Colorimetric method ( $\mu\text{M}$ )	Prepared biosensor ( $\mu\text{M}$ )	Relative deviation (%)
1	317	341	7.57
2	252	259	2.78
3	298	310	4.03
4	482	470	-2.49
5	383	375	-0.26

#### 4. CONCLUSION

In summary, Au NRs@TiO<sub>2</sub> nanocomposite was synthesized successfully and used to construct highly sensitive ECL biosensors for the detection of uric acid. Au NRs@TiO<sub>2</sub> nanocomposite exhibited stable, high intensity ECL property. Because of the excellent ECL properties provided by the Au NRs@TiO<sub>2</sub> nanocomposite, the prepared assay can provide a wide linear range from 40 nM to 28  $\mu\text{M}$  and a low detection limit of 15 nM. The high selectivity, good stability and excellent reproducibility demonstrate that the biosensor could provide a promising method for uric acid detection in clinical diagnosis.

#### ACKNOWLEDGMENTS

This work was supported by Natural Science Foundation of Anhui Province (1808085QB53).

#### References

1. I. Grabowska, M. Chudy, A. Dybko, Z. Brzozka, *Sensor. Actuat. B: Chem.*, 130 (2008) 508.
2. R. Kandár, P. Žáková, V. Muáková, *Clin. Chim. Acta*, 365 (2006) 249.
3. S. M. Usman Ali, N. H. Alvi, B. ZafarI, N. Omer, W. Magnus, D. Bengt, *Sensor. Actuat. B: Chem.*, 152 (2011) 241.
4. R. N. Goyal, V. K. Gupta, M. Oyama, N. Bachheti, *Electrochem. Comm.*, 8 (2006) 65.
5. R. Saravanan, M. M. Khan, V. K. Gupta, E. Mosquera, F. Gracia, V. Narayanan, A. Stephen, *RSC Adv.*, 5 (2015) 34645.
6. E. Liberopoulos, D. Christides, E. Moses, *J. Hypertens.*, 19 (2011) 1855.
7. F. A. Mateos, J. G. Puig, *J. Inherit. Metab. Dis.*, 17 (1994) 138.
8. R. J. Johnson, D. K. Kang, D. Feig, S. Kivlighn, J. Kanellis, S. Watanabe, K. R. Tuttle, B. Rodriguez-Iturbe, J. Herrera-Acosta, M. Mazzali, *Hypertens.*, 41(2013) 1183.
9. M. Alderman, K. J. V. Aiyer, *Curr. Med. Res. Opin.*, 20 (2004) 369.
10. X. Dai, X. Fang, C. Zhang, R. Xu, B. Xu, *J. Chromatogr. B*, 857 (2007) 287.
11. S. K. George, M. T. Dipu, U. R. Mehra, P. Singh, A. K. Verma, J. S. Ramgaokar, *J. Chromatogr. B*, 832 (2006) 134.
12. I. A. Rebelo, J. A. Piedade, A. M. Oliveira-Brett, *Talanta*, 63 (2004) 323.

13. J. F. Jen, S. L. Hsiao, K. H. Liu, *Talanta*, 58 (2002) 711.
14. K. M. Kim, G. N. Henderson, X. Ouyang, R. F. Frye, Y. Y. Sautin, D. I. Feig, R. J. Johnson, *Biomed. Chromatogr.*, 23 (2009) 630.
15. J. Galbán, Y. Andreu, M. J. Almenara, S. De Marcos, J. R. Castillo, *Talanta*, 54 (2001) 847.
16. Y. Li, N. Gong, X. Jiang, X. Zheng, Y. Wang, S. Huan, *J. Chin. Chem. Soc.*, 63 (2016) 660.
17. X. P. Liu, J. Tong, Z. Yuan, Y. Yang, C. J. Mao, H. L. Niu, B. K. Jin, S. Y. Zhang, *J. Nanosci. Nanotechnol.*, 16 (2016) 1645.
18. H. Pan, S. Huang, X. Li, P. Li, W. Zhu, *Int. J. Electrochem. Sci.*, 11 (2016) 3364.
19. X. W. Hu, C. J. Mao, J. M. Song, H. L. Niu, S. Y. Zhang, H. P. Huang, *Biosensor. Bioelectron.*, 41 (2013) 372.
20. S. Huang, G. Pang, X. Li, J. Li, H. Pan, *J. Nanopart. Res.*, 19 (2017) 392.
21. H. Pan, D. Li, J. Liu, J. Li, W. Zhu, Y. Zhao, *J. Phys. Chem. C*, 115 (2011) 14461.
22. S. Wwiss, *Science*, 1999, 283(5408): 1676-1683.
23. Y. Yuan, G. Pang, X. Li, W. Zhu, H. Pan, *Anal. Meth.*, 9 (2017) 5586.
24. S. Nie, S. R. Eniory, *Science*, 275 (1997) 1102.
25. M. Grzelczak, J. Perez-Juste, P. Mulvaney, L. M. LizMarzan, *Chem. Soc. Rev.*, 37 (2008) 1783.
26. Kim, J.; Lee, D. *J. Am. Chem. Soc.*, 129 (2007) 7706 - 7707.
27. L. L. Li, H. Y. Liu, Y. Y. Shen, J.R. Zhang, J. J. Zhu, *Anal. Chem.*, 83 (2011) 661.
28. L. Y. Yu, X. H. Wei, C. Fang, Y. F. Tu, *Electrochim. Acta*, 211 (2016) 27.
29. J. J. Shi, Q. Q. Zhang, W. Hu, P. Yang, *Int. J. Electrochem. Sci.*, 13 (2018) 3575.
30. Y. Yang, L. Qiao, X. P. Liu, P. Z. Liu, C. J. Mao, H. L. Niu, B. K. Jin, S. Y. Zhang, *Electrochim. Acta*, 190 (2016) 948.
31. F. M. Lou, A. J. Wang, J. Jin, Q. F. Li, S. H. Zhang, *Electrochim. Acta*, 278 (2018) 255
32. K. Movlaee, P. Norouzi, H. Beitollahi, M. Rezapour, B. Larijani, *Int. J. Electrochem. Sci.*, 12 (2017) 3241.
33. F.H. Zhang, S. Li, H. Zhang, H.X. Li, G. Li, *Int. J. Electrochem. Sci.*, 12 (2017) 11181.
34. F. Yang, Z. Y. Yu, X. Li, P. P. Ren, G. H. Liu, Y. T. Song, J. Wang, *Spectrochim. Acta A*, 203 (2018) 461.
35. A. Abellan-Llobregat, M. Ayan-Varela, L. Vidal, J.I. Paredes, S. Villar-Rodil, A. Canals and E. Morallon, *J. Electroanal. Chem.* 783 (2016) 41.
36. Y. Wang, Y. Huang, B. Wang, T. Fang, J. Chen and C. Liang, *J. Electroanal. Chem.*, 782 (2016) 76.
37. C. Wang, J. Li, X. Luo, J. Hui, X. Liu, J. Tan and X. Zhao, *J. Electroanal. Chem.*, 780 (2016) 147.
38. Z. Bai, C. Zhou, H. Xu, G. Wang, H. Pang and H. Ma, *Sens. Actuators B*, 243 (2017) 361.